

# Fluctuating pseudoatoms in metallic fluids

Raymond E. Goldstein

*Service de Physique Théorique, Centre d'Etudes Nucléaires de Saclay F-91191 Gif-sur-Yvette Cedex, France and The Enrico Fermi Institute, The University of Chicago, 5640 Ellis Ave., Chicago, Illinois 60637<sup>a)</sup>*

Alberto Parola

*International School for Advanced Studies, 34014 Trieste, Italy*

Arthur P. Smith

*Laboratory of Atomic and Solid State Physics, Cornell University, Ithaca, New York 14853-2501*

(Received 6 February 1989; accepted 20 April 1989)

The nature of long-range many-body interactions in metallic fluids is examined with emphasis on their possible role in the unique features of these systems observed near the liquid-vapor critical point. A reexamination of recent theoretical results demonstrating the existence of van der Waals forces between "pseudoatoms" (ion cores and associated screening electrons) reveals a direct correspondence with dispersion forces in insulating systems. In the limit of high conduction electron number densities  $\rho$ , pseudoatoms have an effective frequency-dependent polarizability  $\alpha(\omega) = \alpha(0)\omega_p^2/(\omega_p^2 - \omega^2)$ , where  $\alpha(0) = z/4\pi\rho$ , with  $z$  the ion valence, and  $\omega_p$  is the classical electron gas plasma frequency  $(4\pi\rho e^2/m)^{1/2}$ . It is the dynamic nature of the interactions (arising from fluctuations of the pseudoatoms) that permits such a long-range interaction to exist. The dimensionless parameter  $\alpha(0)\rho$  which in insulating fluids characterizes the relative importance of triplet (Axilrod-Teller) to pair dispersion interactions is thus system independent and significantly larger than in nonmetallic fluids. The nature of this dynamic polarizability is further examined in the context of a transport theory for a classical plasma based on the Boltzmann equation. The statistical mechanics of fluctuating pseudoatoms at finite temperature is studied both for the metallic fluid and in the Wigner crystal. These various approaches suggest that the pseudoatom interaction may be viewed as a potential mediated by the exchange of plasmons, just as conventional van der Waals forces arise from the exchange of virtual excitations of atomic levels. A description of the critical point in terms of pseudoatom interactions appears to explain qualitatively the extreme liquid-vapor asymmetry of the coexistence curves of cesium and rubidium as arising from the magnitude of three-body interactions. Additionally, it suggests that the thermal energy at the critical point scales with the plasmon energy, consistent with experiment.

## I. INTRODUCTION AND SUMMARY OF RESULTS

An important open problem in the statistical mechanics of fluids is an understanding of liquid-vapor equilibrium in metallic systems. One of the fundamental conceptual difficulties in dealing with such fluids is that the electronic structures of the two phases in equilibrium may be vastly different. For example, far below the critical point the vapor phase is nonmetallic and well characterized by fluctuating dipole (dispersion) interactions. In contrast, the coexisting liquid phase is highly conducting and the interactions are dominated by screened Coulomb potentials. While both of these interactions are sufficiently short ranged so as to lead to critical phenomena typical of insulating fluids, it is the variation of such interactions with thermodynamic state that is difficult to treat and is of central interest.<sup>1</sup> Also in the regime far below the critical point, experimental studies<sup>2</sup> have suggested novel, highly structured interfaces between these two phases. These are quite unlike the monotonically varying density profiles seen in insulating fluids,<sup>3</sup> which are well described by an invariant, pairwise-additive Hamiltonian over the whole of the phase diagram. It has been suggested<sup>4</sup>

that such structuring arises from the density dependence of the interparticle interactions.

Nearer to the liquid-vapor critical point, where the distinctions between coexisting phases vanish, recent thermodynamic and optical studies<sup>5</sup> of the alkali metals cesium and rubidium have shown that metallic behavior is present in both phases; the metal-nonmetal transition appears to occur at a density lower than that of the critical point. It is in this region that there might exist a unified description of the two phases, and the associated critical phenomena.

Recent experiments by Jüngst *et al.*<sup>6</sup> have shown that there are both important similarities and differences between liquid-vapor critical phenomena in insulating and conducting systems. Figure 1 contrasts the coexistence curves of cesium and rubidium in reduced units with that of <sup>3</sup>He.<sup>7</sup> Table I lists the characteristics of those metallic fluids for later reference. Perhaps the most significant feature seen is the extreme *asymmetry of the coexistence curves* of the alkali metals relative to that of <sup>3</sup>He, which is perhaps the most liquid-vapor symmetric of the insulating fluids. Clearly, there is no simple law of corresponding states<sup>8</sup> encompassing both classes of fluids, although the two metals by themselves do follow such a law. Indeed, even in absolute

<sup>a)</sup> Present address.

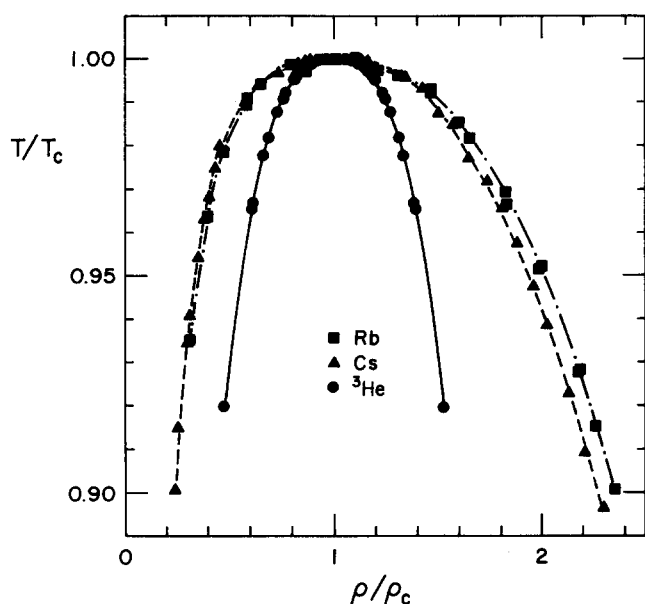


FIG. 1. Liquid-vapor coexistence curves of cesium and rubidium (Refs. 5 and 6) compared with that of  $^3\text{He}$  (Ref. 7). Lines are guides to the eye.

units, Cs and Rb have remarkably similar behavior, their critical temperatures differing by merely 5%. (Note in comparison that the neighboring rare gases in the periodic table, Kr and Xe, have critical temperatures of 209 and 290 K, respectively, differing by nearly 50% from one another.) On the other hand, recent studies<sup>9-11</sup> of critical phenomena in insulating fluids have suggested that the extent of liquid-vapor symmetry may be strongly dependent on the presence of many-body interactions, and that more polarizable fluids characteristically exhibit larger deviations from symmetry. In this respect and others described below, the alkali metals appear to behave as if they were extremely polarizable insulating fluids.

The three-body Axilrod-Teller<sup>12</sup> interaction is the most important of many-body potentials in insulating fluids, and its amplitude, like that of the attractive two-body dispersion force, is governed by the frequency-dependent atomic or molecular polarizability  $\alpha(\omega)$ . The amplitude of the pair interaction, and hence the thermal energy scale at the critical point, is proportional to the frequency integral of  $\alpha^2(\omega)$ . At the same time, the Axilrod-Teller potential scales with the integral of  $\alpha^3(\omega)$ . A convenient measure of the relative im-

portance of such many-body forces at density  $\rho$  is the "polarizability product"  $\alpha(0)\rho$ , and this is the small parameter which appears to control liquid-vapor asymmetry, as well as other nonuniversal aspects of critical phenomena in fluids.

In light of the comments above, one is led naturally to address the corresponding features of liquid-vapor equilibrium in metallic systems: What physical quantities set the energy scale for the critical point, which, as seen in Table I, is thousands of degrees? What small parameter determines the relative size of many-body screened interactions and thus the extent of the liquid-vapor asymmetry? More generally, can a correspondence be made between critical phenomena in insulating and metallic fluids, beyond the universal scaling laws and critical exponents?

Here, we address these questions by studying the quantum statistical mechanics of dispersion forces in metallic fluids, focusing on the interactions between "pseudoatoms."<sup>13</sup> These entities may roughly be described as ions and their associated screening electrons, and arise from the coupling of the ions to the bulk plasmons. As such, their existence derives from the properties of the interacting electron gas, and not from electrons bound to the ions. Central to the analysis is a reinterpretation of recent theoretical results<sup>14,15</sup> demonstrating in high-order many-body perturbation theory that such pseudoatoms interact with attractive forces of the same asymptotic power-law decay as in conventional van der Waals forces between neutral, polarizable atoms, namely as (distance)<sup>-6</sup>, but pertaining entirely to the metallic state.

Our reinterpretation, based on a systematic study of the perturbation theory (Sec. II), supporting arguments from a transport equation study (Sec. III), an analysis of analogous phenomena in the Wigner crystal (Sec. IV), and finite-temperature generalizations of the pseudoatom interaction (Sec. V), reveals that pseudoatoms may be characterized at zero temperature by a frequency-dependent polarizability

$$\alpha(\omega) = \alpha(0) \frac{\omega_p^2}{\omega_p^2 - \omega^2} \quad (1.1)$$

with a static value

$$\alpha(0) = \frac{z}{4\pi\rho_e}, \quad (1.2)$$

where  $z$  is the ionic valence,  $\rho_e$  is the electron number density, and with an excitation frequency equal to the classical electron gas plasma frequency

$$\omega_p \equiv \left( \frac{4\pi\rho_e e^2}{m} \right)^{1/2}, \quad (1.3)$$

with  $m$  the electron mass. The finite-temperature corrections to these zero-temperature results, exhibiting a gap in the excitation spectrum equal to the energy level spacing of the plasmon modes, suggest that the pseudoatoms interact by virtual plasmon excitations,<sup>15</sup> much as ordinary atoms interact by virtual excitations of core levels. The simple form of the pseudoatom polarizability, involving only a single excitation frequency (in contrast to the case in atoms in which virtual excitations may occur to a large number of excited states), arises essentially from the selection rules for transi-

TABLE I. Measured and derived critical properties of the alkali metals, after Ref. 6.

	Cs	Rb
$T_c$ (K)	1924	2017
$\rho_c$ ( $\text{\AA}^{-3}$ )	0.001 72	0.002 06
$r_s(\rho_c)$ ( $\text{\AA}$ )	5.18	4.88
$k_F^{-1}(\rho_c)$ ( $\text{\AA}$ )	2.70	2.54
$k_{TF}^{-1}(\rho_c)$ ( $\text{\AA}$ )	1.06	1.03
$\hbar\omega_p(\rho_c)$ (eV)	1.54	1.68
$k_B T_c / \hbar\omega_p(\rho_c)$	0.108	0.103

tions between states of a harmonic oscillator, representing in this case the plasmons.

From Eqs. (1.1) and (1.2) we find that the pseudoatom pair interaction is

$$\phi(r) = -\frac{3}{4}\hbar\omega_p \frac{(1/4\pi\rho)^2}{r^6}, \quad (1.4)$$

while the triplet analog of the Axilrod-Teller potential is

$$\psi(r_1, r_2, r_3) = \frac{9}{16}\hbar\omega_p (1/4\pi\rho)^3 \times \frac{[3 \cos(\theta_1)\cos(\theta_2)\cos(\theta_3) + 1]}{r_{12}^3 r_{13}^3 r_{23}^3}. \quad (1.5)$$

Together, these imply that the small parameter controlling the importance of many-body interactions is a system-independent quantity,  $1/4\pi$ , in the limit of high densities. As discussed in Sec. VI, this "universality" of the polarizability product and its magnitude suggest the origin of the remarkable similarity of the phase diagrams of the metallic systems and their significant departure from those of insulators. At the same time, the pseudoatom interactions provide a possible relation between the thermal energy at the critical point and the plasmon energy, one that is qualitatively consistent with the experimental data. A detailed discussion of recent thermodynamic studies of expanded alkali metals is considered in later work.<sup>16</sup>

## II. PSEUDOATOM INTERACTIONS AT ZERO TEMPERATURE

### A. The Hamiltonian

It is useful first to describe the underlying Hamiltonian of a metallic fluid of polarizable ionic cores in an interacting electron gas.<sup>17-19</sup> Consider a fluid composed of  $N$  ion cores of atomic number  $Z$  and charge  $z$ , with coordinates  $\{\mathbf{R}_i\}$ , each with  $z_c \equiv Z - z$  bound core electrons described by the vectors  $\{r_{ij}\}$  relative to the nucleus. The total charge density is denoted by  $c(\mathbf{r})$ ,

$$c(\mathbf{r}) = e \left\{ \sum_{i=1}^N \left[ Z\delta(\mathbf{r} - \mathbf{R}_i) - \sum_{j=1}^{z_c} \delta(\mathbf{r} - \mathbf{R}_i - \mathbf{r}_{ij}) \right] - \sum_{k=1}^{zN} \delta(\mathbf{r} - \mathbf{r}_k) \right\}, \quad (2.1)$$

where the vectors  $\mathbf{r}_k$  label the coordinates of the free electrons, and has a Fourier transform

$$\hat{c}(\mathbf{q}) \equiv \hat{\rho}(\mathbf{q}) + \hat{n}(\mathbf{q}) + \hat{\tau}(\mathbf{q}), \quad (2.2)$$

where

$$\hat{\rho}(\mathbf{q}) = ze \sum_{i=1}^N e^{-iq \cdot \mathbf{R}_i}, \quad \hat{n}(\mathbf{q}) = -e \sum_{k=1}^{zN} e^{-iq \cdot \mathbf{r}_k} \quad (2.3)$$

describes the density of cores, viewed as point ions, and of free electrons, and

$$\hat{\tau}(\mathbf{q}) = e \sum_{i=1}^N e^{-iq \cdot \mathbf{R}_i} \sum_{j=1}^{z_c} (1 - e^{-iq \cdot \mathbf{r}_{ij}}) \quad (2.4)$$

accounts for the fluctuations of the core electrons.

In a perturbation theory which treats the reference system as the noninteracting homogeneous electron gas, we therefore consider the full perturbing Hamiltonian,

$$\mathcal{H}_1 = \int \frac{d^3q}{(2\pi)^3} \{ \hat{\mathcal{H}}_{\tau\tau} + \hat{\mathcal{H}}_{nn} + \hat{\mathcal{H}}_{\rho\tau} + \hat{\mathcal{H}}_{\rho n} + \hat{\mathcal{H}}_{\tau n} \}, \quad (2.5)$$

where

$$\hat{\mathcal{H}}_{\tau\tau} = \frac{1}{2} \hat{\tau}(\mathbf{q}) \hat{\tau}(-\mathbf{q}) \hat{v}_c(\mathbf{q}), \quad \hat{\mathcal{H}}_{nn} = \frac{1}{2} \hat{n}(\mathbf{q}) \hat{n}(-\mathbf{q}) \hat{v}_c(\mathbf{q}), \quad (2.6)$$

$$\hat{\mathcal{H}}_{\rho\tau} = \hat{\rho}(\mathbf{q}) \hat{\tau}(-\mathbf{q}) \hat{v}_c(\mathbf{q}), \quad \hat{\mathcal{H}}_{\rho n} = \hat{\rho}(\mathbf{q}) \hat{n}(-\mathbf{q}) \hat{v}_c(\mathbf{q}), \quad (2.7)$$

and

$$\hat{\mathcal{H}}_{\tau n} = \hat{\tau}(\mathbf{q}) \hat{n}(-\mathbf{q}) \hat{v}_c(\mathbf{q}), \quad (2.8)$$

where the Fourier transform of the Coulomb interaction is  $\hat{v}_c(\mathbf{q}) = 4\pi/q^2$ .

The derivation of the pseudoatom interaction at zero temperature employs standard time-ordered Goldstone perturbation theory<sup>20</sup> in which the  $n$ th order contribution to the energy is computed as

$$E_{n_\alpha n_\beta \dots}^{(n)} = \frac{(-i/\hbar)^{n-1}}{n_\alpha! n_\beta! \dots} \int dt_1 \dots \int dt_{n-1} \times \langle \Psi_0 | T \{ \hat{\mathcal{H}}_1^{\alpha} \hat{\mathcal{H}}_1^{\alpha}(t_1) \dots \hat{\mathcal{H}}_1^{\alpha}(t_{n_\alpha-1}) \times \hat{\mathcal{H}}_1^{\beta}(t_{n_\alpha}) \dots \hat{\mathcal{H}}_1^{\beta}(t_{n_\alpha+n_\beta-1}) \dots \} | \Psi_0 \rangle_c, \quad (2.9)$$

where  $\alpha$  and  $\beta$  label the terms within  $\mathcal{H}_1$ ,  $T$  is the time-ordering operator,  $\Psi_0$  is the ground state of the noninteracting system, and the subscript  $c$  denotes connected diagrams. It may be assumed<sup>17</sup> that  $\Psi_0$  is a product of the ground state of the noninteracting electron gas and a set of localized atomic core states  $\Phi_{\mathbf{R}}$  describing an ion at position  $\mathbf{R}$ .

### B. van der Waals interactions between atoms

Let us first review for the purposes of later comparison the computation of van der Waals forces between atoms with fluctuating bound electrons.<sup>17</sup> These are obtained by considering the perturbation  $\hat{\mathcal{H}}_{\tau\tau}$  to second order, with the result

$$E_{\tau\tau}^{(2)} = \frac{1}{2!} \sum_{\mathbf{R} \neq \mathbf{R}'} \phi_{2\tau\tau}(|\mathbf{R} - \mathbf{R}'|), \quad (2.10)$$

where the pair interaction is

$$\phi_{2\tau\tau}(r) = -\hbar \int_0^\infty \frac{d\omega}{2\pi} \int \frac{d^3q}{(2\pi)^3} \int \frac{d^3q'}{(2\pi)^3} \bar{D}_{\mathbf{R}}(\mathbf{q}, \mathbf{q}', i\omega) \times \bar{D}_{\mathbf{R}'}(-\mathbf{q}, -\mathbf{q}', -i\omega) \hat{v}_c(\mathbf{q}) \hat{v}_c(\mathbf{q}'). \quad (2.11)$$

Here,  $\bar{D}_{\mathbf{R}}$ , represented by the ovals in Fig. 2(a), is the temporal Fourier transform of the core fluctuation operator

$$\hat{D}_{\mathbf{R}}(\mathbf{q}, \mathbf{q}', t_2 - t_1) \equiv (-i/\hbar) \langle \Phi_{\mathbf{R}} | T \times \{ \hat{\tau}_{\mathbf{R}}(\mathbf{q}, t_1) \hat{\tau}_{\mathbf{R}}(-\mathbf{q}', t_2) \} | \Phi_{\mathbf{R}} \rangle, \quad (2.12)$$

where the wave functions  $\Phi_{\mathbf{R}}$  of the bound electrons have been assumed to be localized on a scale smaller than the mean interparticle spacing.

Since we are interested in interactions on a scale large compared to the core size, we use the long-wavelength ("dipole") approximation,

$$\bar{D}_{\mathbf{R}}(\mathbf{q}, \mathbf{q}', \omega) \simeq -e^{-i(\mathbf{q} - \mathbf{q}') \cdot \mathbf{R}} \alpha(\omega) [\mathbf{q} \cdot \mathbf{q}'], \quad (2.13)$$

where

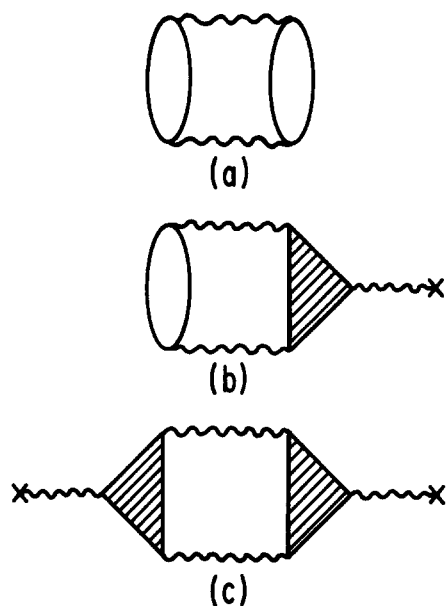


FIG. 2. Two-body interactions in perturbation theory. Diagrams illustrate the van der Waals interaction between two polarizable atoms (a), an atom and a pseudoatom (b), and two pseudoatoms (c). Wiggly lines represent (possibly) screened Coulomb interactions, ovals represent the atomic polarizability, and shaded triangles stand for the three-point function of the electron gas.

$$\alpha(\omega) = \frac{2}{3} \frac{e^2}{\hbar} \sum_n \frac{\omega_n |\langle n | \Sigma \mathbf{r} | 0 \rangle|^2}{\omega_n^2 - \omega^2} \quad (2.14)$$

is the atomic polarizability, expressed in terms of the matrix elements of the total electric dipole operator (a sum over all bound electrons) between the ground state  $|0\rangle$  and the bound states  $|n\rangle$ . Use of the identity

$$\int \frac{d^3q}{(2\pi)^3} \int \frac{d^3q'}{(2\pi)^3} e^{-i(\mathbf{q}-\mathbf{q}') \cdot \mathbf{r}} \hat{f}(q) \hat{f}(q') [\mathbf{q} \cdot \mathbf{q}']^2 = \left(\frac{d^2f}{dr^2}\right)^2 + \frac{2}{r^2} \left(\frac{df}{dr}\right)^2 \quad (2.15)$$

with the Coulomb potential yields  $6/r^6$ , so

$$\phi_{2\tau\tau}(r) = -6 \left[ \hbar \int_0^\infty \frac{d\omega}{2\pi} \alpha(i\omega)^2 \right] \frac{1}{r^6} \quad (2.16)$$

If we approximate the sum in Eq. (2.14) by the contribution from a single level with frequency  $\Delta$ , then

$$\alpha(\omega) \simeq \frac{\alpha(0)\Delta^2}{\Delta^2 - \omega^2} \quad (2.17)$$

and

$$\phi_{2\tau\tau}(r) = -\frac{3}{4} \frac{\hbar \Delta \alpha(0)^2}{r^6} \quad (2.18)$$

Thus, the amplitude of the  $1/r^6$  interaction is determined by two parameters, the zero-frequency polarizability  $\alpha(0)$  and the characteristic excitation frequency  $\Delta$ .

Considering the third-order perturbation result for the term  $\mathcal{H}_{\tau\tau}$  [Fig. 3(a)], we obtain the three-body contribution to the energy

$$E_{\tau\tau}^{(3)} = \frac{1}{3!} \sum_{\mathbf{R} \neq \mathbf{R}' \neq \mathbf{R}''} \psi_{3\tau\tau}(\mathbf{R}, \mathbf{R}', \mathbf{R}''), \quad (2.19)$$

where the triplet potential is

$$\begin{aligned} \psi_{3\tau\tau}(\mathbf{R}, \mathbf{R}', \mathbf{R}'') &= -2\hbar \int_0^\infty \frac{d\omega}{2\pi} \int \frac{d^3q}{(2\pi)^3} \int \frac{d^3q'}{(2\pi)^3} \int \frac{d^3q''}{(2\pi)^3} \\ &\quad \times \tilde{D}_{\mathbf{R}}(\mathbf{q}, \mathbf{q}', i\omega) \tilde{D}_{\mathbf{R}'}(-\mathbf{q}, -\mathbf{q}'', -i\omega) \\ &\quad \times \tilde{D}_{\mathbf{R}''}(\mathbf{q}', \mathbf{q}'', i\omega) \hat{v}_c(\mathbf{q}) \hat{v}_c(\mathbf{q}') \hat{v}_c(\mathbf{q}''). \end{aligned} \quad (2.20)$$

Within the dipole approximation, the necessary identity analogous to Eq. (2.15) in the case of the triplet interaction is

$$\begin{aligned} &\int \frac{d^3q}{(2\pi)^3} \int \frac{d^3q'}{(2\pi)^3} \int \frac{d^3q''}{(2\pi)^3} e^{-i(\mathbf{q}-\mathbf{q}') \cdot \mathbf{R}'} e^{-i(\mathbf{q}''-\mathbf{q}') \cdot \mathbf{R}''} \\ &\quad \times e^{-i(\mathbf{q}'-\mathbf{q}'') \cdot \mathbf{R}''} \hat{f}(q) \hat{f}(q') \hat{f}(q'') (\mathbf{q} \cdot \mathbf{q}') (\mathbf{q} \cdot \mathbf{q}'') (\mathbf{q}' \cdot \mathbf{q}'') \\ &= 3 \frac{[3 \cos(\theta_1) \cos(\theta_2) \cos(\theta_3) + 1]}{r_{12}^3 r_{13}^3 r_{23}^3} \\ &\equiv 3\Theta_{AT}(\{\theta_i\}, \{r_i\}), \end{aligned} \quad (2.21)$$

where the  $\theta_i$  are the interior angles of the triangle formed by the three vectors  $(\mathbf{R}, \mathbf{R}', \mathbf{R}'')$  and the  $r_{ij}$  are the triangle leg lengths. Combining these results, we obtain

$$\begin{aligned} \psi_{3\tau\tau}(r_1, r_2, r_3) &= 6 \left[ \hbar \int_0^\infty \frac{d\omega}{2\pi} \alpha(i\omega)^3 \right] \Theta_{AT}(\{\theta_i\}, \{r_i\}) \\ &= \frac{9}{16} \hbar \Delta \alpha(0)^3 \Theta_{AT}(\{\theta_i\}, \{r_i\}) \end{aligned} \quad (2.22)$$

in the single-level approximation.

### C. van der Waals interactions between pseudoatoms

Following previous work,<sup>14</sup> let us now consider the fourth-order diagram shown in Fig. 2(c). It represents the interaction between two ions mediated by the two three-point functions (nonlinear response functions) of the electron gas, represented by the shaded triangles. In contrast to the more familiar linear processes by which exponentially screened interactions arise, namely the charge density induced by an ion interacting directly with the Coulomb field of another, the process depicted in Fig. 2 is inherently nonlinear. It may be viewed as a second-order interaction between two inhomogeneous screening clouds, the inhomogeneities arising from a linear coupling of the electron gas to the ionic Coulomb potentials.

To evaluate the potential implied by Fig. 2(c), we approximate the ion-conduction electron interaction (the combination of the terms  $\hat{\mathcal{H}}_{\rho n}$  and  $\hat{\mathcal{H}}_{\tau n}$ ) by a pseudopotential  $v_{ps}(r)$ , treating the electron gas as only weakly inhomogeneous. In the analysis below we focus only on the long-wavelength properties of the ion-ion interaction, so the detailed form of the pseudopotential need not be specified. The effects of electron-electron screening of the Coulomb interactions on the interion potential are accounted for through the dielectric function  $\epsilon(q, \omega)$ , and lead to the pseudoatom interaction

$$\phi_{2\text{pseudo}}(r) = -\hbar \int_0^\infty \frac{d\omega}{2\pi} \int \frac{d^3q}{(2\pi)^3} \int \frac{d^3q'}{(2\pi)^3} e^{-i(\mathbf{q}-\mathbf{q}')\cdot\mathbf{R}} e^{-i(\mathbf{q}'-\mathbf{q})\cdot\mathbf{R}'} \left[ \frac{e^4 \hat{v}_{ps}(|\mathbf{q}-\mathbf{q}'|) \tilde{S}(\mathbf{q}'-\mathbf{q}, 0, \mathbf{q}, i\omega, -\mathbf{q}', -i\omega)}{\hbar^2 \epsilon(|\mathbf{q}-\mathbf{q}'|, 0) \epsilon(\mathbf{q}, i\omega)} \right] \\ \times \left[ \frac{e^4 \hat{v}_{ps}(|\mathbf{q}'-\mathbf{q}|) \tilde{S}(\mathbf{q}-\mathbf{q}', 0, -\mathbf{q}, -i\omega, -\mathbf{q}', i\omega)}{\hbar^2 \epsilon(|\mathbf{q}'-\mathbf{q}|, 0) \epsilon(\mathbf{q}', i\omega)} \right] \hat{v}_c(q) \hat{v}_c(q'). \quad (2.23)$$

Note the formal resemblance to Eq. (2.11), with the quantities in large parentheses playing the role of the product  $\alpha(\omega)\mathbf{q}\cdot\mathbf{q}'$  in the dipole approximation (2.13).

The quantity  $\tilde{S}$  is related to the three-point function of the electron gas by the following: Define

$$\Upsilon^{(3)}(\mathbf{r}_1, t_1, \mathbf{r}_2, t_2, \mathbf{r}_3, t_3) \\ \equiv (-i) \langle T \{ n(\mathbf{r}_1, t_1) n(\mathbf{r}_2, t_2) n(\mathbf{r}_3, t_3) \} \rangle, \quad (2.24)$$

as the time-order expectation of the electron number operators. This function has a spatial and temporal Fourier transform which satisfies

$$\tilde{\Upsilon}^{(3)}(\mathbf{q}_1, \omega_1, \mathbf{q}_2, \omega_2, \mathbf{q}_3, \omega_3) \\ = (2\pi)^4 \delta(\mathbf{q}_1 + \mathbf{q}_2 + \mathbf{q}_3) \delta(\omega_1 + \omega_2 + \omega_3) \\ \times \tilde{S}(\mathbf{q}_1, \omega_1, \mathbf{q}_2, \omega_2, -\mathbf{q}_1 - \mathbf{q}_2, -\omega_1 - \omega_2). \quad (2.25)$$

The lowest-order expression for the function  $\tilde{S}$ , valid in the noninteracting electron gas at high densities, involves only zeroth order free-electron Green's functions:

$$\tilde{S}(\mathbf{q}_1, \omega_1, \mathbf{q}_2, \omega_2, -\mathbf{q}_1 - \mathbf{q}_2, -\omega_1 - \omega_2) \\ = 2 \int \frac{d^3k}{(2\pi)^3} \int \frac{d\omega}{2\pi} [\tilde{G}^0(\mathbf{k}, \omega) \tilde{G}^0(\mathbf{k} + \mathbf{q}_2, \omega + \omega_2) \\ \times \tilde{G}^0(\mathbf{k} - \mathbf{q}_1, \omega - \omega_1) + \tilde{G}^0(\mathbf{k}, \omega) \\ \times \tilde{G}^0(\mathbf{k} - \mathbf{q}_2, \omega - \omega_2) \tilde{G}^0(\mathbf{k} + \mathbf{q}_1, \omega + \omega_1)], \quad (2.26)$$

where

$$\tilde{G}^0(\mathbf{k}, \omega) = \left\{ \frac{\theta(k - k_F)}{\omega - \omega_k + i\eta} + \frac{\theta(k_F - k)}{\omega - \omega_k - i\eta} \right\}, \quad (2.27)$$

$\eta$  being a positive infinitesimal.

A complete evaluation of the frequency and momentum integrals in Eq. (2.23) requires knowledge of the three-point function for the full range of its arguments. In the original study of the pseudoatom interactions,<sup>14</sup> a high-frequency approximation to  $\tilde{S}$  and the dielectric function was employed; subsequent calculations<sup>15</sup> have shown that certain singularities in these functions lead to small logarithmic corrections to the pseudoatom potential. In what follows, we employ the high-frequency approximation in order to demonstrate the correspondence between real and pseudoatom interactions, reserving a more complete discussion for later work.<sup>16</sup> Note that both statically and dynamically screened Coulomb interactions appear in the diagram; this caveat applies only to the internal dynamically screened Coulomb lines.

As with the dispersion force arising from bound core electrons, we focus attention on the long-range behavior of the pseudoatom interaction, and therefore examine the integrand in Eq. (2.23) in the limit of small momenta. The separate contributions to Eq. (2.23) in the limit of small momenta  $\mathbf{q}$  and  $\mathbf{q}'$  and at high frequencies may now be enumerated. The three-point function has the simple form

$$\tilde{S}(\mathbf{q} - \mathbf{q}', 0, -\mathbf{q}, -i\omega, \mathbf{q}', i\omega) \simeq i \frac{k_F}{\pi^2} \frac{\mathbf{q}\cdot\mathbf{q}'}{\omega^2}, \quad (2.28)$$

where  $k_F$  is the Fermi wave vector of the electron gas. The zero-frequency dielectric constant screens out the divergent Coulomb form of the pseudopotential

$$\lim_{q \rightarrow 0} \frac{\hat{v}_{ps}(q)}{\epsilon(q, 0)} \simeq \frac{4\pi z}{k_{sc}^2}, \quad (2.29)$$

where  $k_{sc}$  is the screening wave vector. Continuing to treat the electron gas in the high-density limit, we treat the screening within the Thomas-Fermi approximation, obtaining the zero-temperature result

$$k_{sc} \simeq k_{TF} = \left( \frac{6\pi z \rho e^2}{\epsilon_F} \right)^{1/2}, \quad (2.30)$$

with  $\epsilon_F$  the Fermi energy. Finally, the long-wavelength finite-frequency dielectric constant is obtained from the plasmon result,

$$\lim_{q \rightarrow 0} \epsilon(q, \omega) \simeq 1 - (\omega_p^2 / \omega^2). \quad (2.31)$$

Combining these results, we obtain the attractive fluctuating pseudoatom interaction

$$\phi_{2\text{pseudo}}(r) = -\frac{3}{4} \hbar \omega_p \frac{(1/4\pi\rho)^2}{r^6}. \quad (2.32)$$

We have written Eq. (2.32) in a form which emphasizes our interpretation of the pseudoatoms, for by comparison with Eq. (2.18) we may draw the correspondences

$$\alpha(o) \rightarrow \frac{1}{4\pi\rho}, \quad \Delta \rightarrow \omega_p \quad (2.33)$$

with the potential Eq. (2.18) for insulating fluids. These identifications remain valid when extended to the triplet pseudoatom interaction illustrated in Fig. 3(d). Using the high-frequency approximations described above, we find the Axilrod-Teller interaction given in Eq. (1.5).

Recall that in identifying the pseudoatom polarizability as

$$\alpha_{\text{pseudo}}(\omega) = \left( \frac{1}{4\pi\rho} \right) \frac{\omega_p^2}{\omega_p^2 - \omega^2} \quad (2.34)$$

we have included the contribution from the dielectric function associated with one of the screened internal Coulomb lines of the diagram. If we consider now the pair interaction between a pseudoatom and a neutral, polarizable atom as shown in Fig. 2(b), we may clarify this association. Within the single-level approximation we find this potential to be

$$\phi(r) = -\frac{3}{4} \hbar \omega_p \left( \frac{1}{4\pi\rho} \right) \alpha(0) \left( \frac{\Delta}{\Delta + \omega_p} \right)^2 \frac{1}{r^6}. \quad (2.35)$$

Comparing this result to the interaction between two different neutral atoms, with polarizabilities  $\alpha_v(\omega) = \alpha_v(0) \Delta_v^2 /$

$(\Delta^2 - \omega^2)$ , for  $\nu = A, B$ , and in which only one of the Coulomb lines is dynamically screened, we find

$$\phi_{AB}(r) = -\frac{3}{2} \hbar \alpha_A(0) \alpha_B(0) \times \frac{\Delta_A^2 \Delta_B^2}{(\Delta_A + \Delta_B)(\Delta_A + \omega_p)(\Delta_B + \omega_p)} \frac{1}{r^6}. \quad (2.36)$$

Setting  $\Delta_B \equiv \omega_p$  and  $\alpha_B(0) \equiv 1/4\pi\rho$ , we obtain precisely Eq. (2.35).

In addition to the triple-pseudoatom potential, there are two long-range triplet interactions involving both pseudoatoms and polarizable cores, as shown diagrammatically in Figs. 3(b) and 3(c). All have the same real-space functional form; they differ only in their amplitudes. If we define amplitudes  $A_i$  such that for the unscreened Axilrod-Teller interaction  $A = \hbar\Delta\alpha(0)^3$ , then we find the fully screened amplitudes associated with the diagrams in Fig. 3 to be

$$\begin{aligned} A_a &= \hbar\Delta\alpha(0)^3 \left( \frac{\Delta}{\Delta + \omega_p} \right)^5, \\ A_b &= \frac{4}{3} \hbar\omega_p\alpha(0)^2 \left( \frac{1}{4\pi\rho} \right) \left( \frac{\Delta}{\Delta + \omega_p} \right)^3, \\ A_c &= \frac{1}{3} \hbar\omega_p\alpha(0) \left( \frac{1}{4\pi\rho} \right)^2 \frac{\Delta^2(\Delta + 3\omega_p)}{(\Delta + \omega_p)^3}, \\ A_d &= \hbar\omega_p \left( \frac{1}{4\pi\rho} \right)^3, \end{aligned} \quad (2.37)$$

The relative importance of the pseudoatom interactions to those between polarizable cores may be found simply by comparing the amplitudes of the respective  $r^{-6}$  potentials. We find that the fluctuating pseudoatom pair interactions will dominate the core van der Waals attraction at sufficiently low densities, since the product  $\omega_p/\rho^2$  scales as  $\rho^{-3/2}$ . Analytically, the pseudoatom-pseudoatom interaction is larger than the core-core potential provided

$$\rho < 0.38\Delta^{-2/3}\alpha(0)^{-4/3}, \quad (2.39)$$

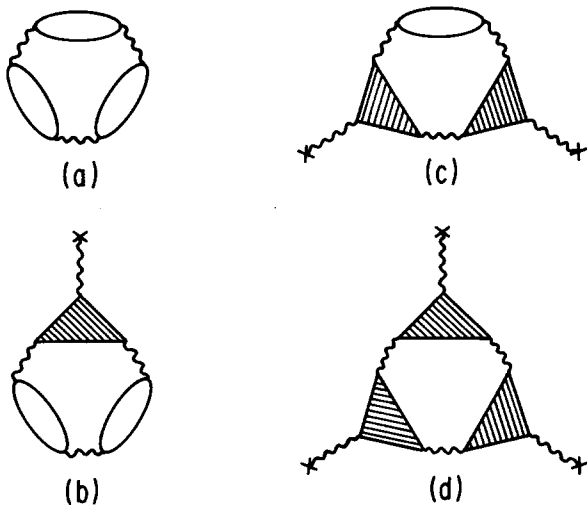


FIG. 3. As in Fig. 2, but for the three-body interactions involving atoms and pseudoatoms.

where  $\rho$  is expressed in  $\text{\AA}^3$ ,  $\Delta$  in eV, and  $\alpha(0)$  in  $\text{\AA}^3$ . For example when  $\alpha(0) = 3 \text{\AA}^3$  and  $\Delta = 10$  eV, we find that the pseudoatom interactions dominate the core ones for all electron densities less than about  $0.02 \text{\AA}^{-3}$ , an order of magnitude larger than the critical densities of the alkali metals.

### III. FLUCTUATING PSEUDOATOMS FROM RESPONSE THEORY

The results in the previous section for the interactions between pseudoatoms show that both the static polarizability  $\alpha(0) = 1/4\pi\rho$  and the excitation frequency  $\Delta = \omega_p$  are purely classical quantities. As such, one would expect that they should arise purely within the context of a classical treatment, without resort to the formally high-order quantum many-body perturbation theory used above. Here, we demonstrate that the high-frequency form of the pseudoatom polarizability may also be obtained from the Boltzmann equation in a classical plasma.<sup>21</sup> Note, however, that the finite-temperature treatments discussed in Secs. IV and V suggest that the  $1/r^6$  interaction itself, arising from the pseudoatom polarizability, appears to be inherently quantum mechanical (for example, the amplitude contains the factor  $\hbar\omega_p$ ).

Consider a high-temperature, nondegenerate, low-density electron gas with a fixed ionic impurity of charge  $+ze$  embedded in it. We determine the time-dependent dipole moment induced in the system upon the application of a uniform oscillating electric field  $\mathbf{E}(t) = \mathbf{E}_0 e^{-i\omega t}$ , and thereby find the frequency-dependent polarizability. In the absence of a field, the effective ionic potential  $\phi$  is a Coulomb potential screened by the surrounding plasma, and it is this spherically symmetric screening cloud which is distorted by the probe field  $\mathbf{E}$ . We seek the distribution function  $f(\mathbf{r}, \mathbf{p}, t)$  describing the time-dependent phase-space probability density for electrons at position  $\mathbf{r}$  with momentum  $\mathbf{p}$ , and develop  $f$  perturbatively,

$$f(\mathbf{r}, \mathbf{p}, t) = f_0 + f_\phi + f_E + f_{\phi E} + \dots, \quad (3.1)$$

where  $f$  is the exact distribution function,

$$f_0(\mathbf{p}) = \rho_0 (2\pi m k_B T)^{-3/2} \exp(-p^2/2mk_B T),$$

is the unperturbed distribution function for the plasma,  $f_\phi$  is linear in  $\phi$ , etc., and  $f_{\phi E}$  is of quadratic order. The electron number density  $\rho_0$  is here taken to be that associated with a background positive ion density  $\rho$  as in the preceding section, so that  $\rho_0 = z\rho$ .

For clarity here, we shall use the collisionless Boltzmann equation. This collisionless assumption is valid<sup>22</sup> in the high-frequency limit  $\omega \gg \tau^{-1}$  where  $\tau$  is the effective scattering time. The Boltzmann equation itself is only valid in a nearly ideal plasma, which requires that the Debye-Huckel screening length  $\lambda_{\text{DH}} = \sqrt{(kT/4\pi e^2 \rho_0)}$  be longer than the mean interparticle spacing. This means the method can be trusted only at high temperatures or relatively low densities. With the potential  $\phi$  determined self-consistently from the inhomogeneities of the plasma we arrive at the Vlasov equation,

$$\frac{\partial f}{\partial t} + \mathbf{v} \cdot \nabla f + e(\nabla\phi - \mathbf{E}) \cdot \frac{\partial f}{\partial \mathbf{p}} = 0. \quad (3.2)$$

Substituting Eq. (3.1) into Eq. (3.2), we obtain the linear response results for  $f_\phi$  and  $f_E$ ,

$$f_\phi(\mathbf{r}, \mathbf{p}) = \beta e^2 \phi(r) f_0(p) \quad (3.3)$$

and

$$f_E(\mathbf{r}, \mathbf{p}) = \frac{e^2}{-i\omega} \mathbf{E} \cdot \frac{\partial f_0}{\partial \mathbf{p}}. \quad (3.4)$$

Integrating  $f_\phi$  over momentum yields the shift in density  $\rho_\phi(r) = \rho_0 \beta e^2 \phi(r)$ , which, when solved along with the Poisson equation,  $\nabla^2 \phi(r) = -4\pi \rho(r)$ , gives the usual Debye-Huckel screened potential

$$\phi(r) = \frac{ze}{r} e^{-r/\lambda_{DH}}. \quad (3.5)$$

Taking the bilinear term to be of the form  $g_{\phi E}(\mathbf{r}, \mathbf{p}) e^{-i\omega t}$  we find

$$\left(-i\omega + \frac{\mathbf{p} \cdot \nabla}{2m}\right) g_{\phi E} = \frac{\beta e^2}{m} \phi(r) \mathbf{E}_0 \cdot \mathbf{p} \frac{\partial f_0}{\partial \epsilon} + \frac{e^2}{im\omega} (\nabla \phi) \cdot \frac{\partial}{\partial \mathbf{p}} \left( \mathbf{E}_0 \cdot \mathbf{p} \frac{\partial f_0}{\partial \epsilon} \right), \quad (3.6)$$

where  $\epsilon = p^2/2m$ .

In Fourier space, with  $\hat{\phi}(\mathbf{q}) = \int d^3r e^{-i\mathbf{q}\cdot\mathbf{r}} \phi(\mathbf{r})$ , etc., we find

$$\hat{g}_{\phi E}(\mathbf{q}, \mathbf{p}) = \frac{\beta e^2 \hat{\phi}(\mathbf{q})}{-im\omega} (\mathbf{E}_0 \cdot \mathbf{p}) \frac{\partial f_0}{\partial \epsilon} - \frac{i\hat{\phi}(\mathbf{q}) e^2}{\omega(\mathbf{p}\cdot\mathbf{q} - m\omega)} (\mathbf{q} \cdot \mathbf{E}_0) \frac{\partial f_0}{\partial \epsilon}. \quad (3.7)$$

To determine the induced dipole moment, we first integrate  $\hat{g}_{\phi E}$  over momentum to obtain the Fourier transform  $\hat{n}_{\phi E}(\mathbf{q})$  of the real-space distribution. The first term in Eq. (3.7) integrates to zero by the symmetry of  $f_0$ , and in the limit of small  $\mathbf{q}$  we find

$$\hat{n}_{\phi E}(\mathbf{q}) = -\frac{\beta e^2 \rho_0}{m\omega^2} i\mathbf{q} \cdot \mathbf{E}_0 \hat{\phi}(\mathbf{q}). \quad (3.8)$$

This, in turn, implies

$$n_{\phi E}(\mathbf{r}) = -\frac{\beta e^2 \rho_0}{m\omega^2} \mathbf{E}_0 \cdot \nabla \phi(r) \quad (3.9)$$

to order  $q^2/\omega^2$ . From this, we obtain the induced dipole moment

$$\mathbf{d} = -e \int d^3r \mathbf{r} n_{\phi E}(\mathbf{r}) = -z\beta\lambda_{DH}^2 \frac{\omega_p^2}{\omega^2} \mathbf{E}_0 \quad (3.10)$$

equivalent to a polarizability

$$\alpha(\omega) = -\frac{z}{4\pi\rho_0} \frac{\omega_p^2}{\omega^2}, \quad (3.11)$$

in the limit of high frequencies, which is just the high-frequency limit of the pseudoatom polarizability Eq. (2.34).

The effects of a finite scattering time on the pseudoatom polarizability may be studied by generalizing the collisionless Boltzmann equation to include scattering processes. Consider the incorporation of such terms within a relaxation-time approximation, giving the evolution equation

$$\frac{\partial f}{\partial t} + \mathbf{v} \cdot \nabla f + e(\nabla \phi - \mathbf{E}) \cdot \frac{\partial f}{\partial \mathbf{p}} = -\frac{[f - (f_0 + f_\phi)]}{\tau}, \quad (3.12)$$

with  $\tau$  the relaxation time. The form of the right-hand side in Eq. (3.12) is such as to drive  $f(\mathbf{r}, \mathbf{p}, t)$  to the local equilibrium distribution determined to linear order in the screened potential  $\phi$ . Carrying through the analysis as above, we find the polarizability modified by the finite relaxation time to be

$$\alpha(\omega) = -\frac{z}{4\pi\rho_0} \frac{\omega_p^2}{\omega^2 - 1/\tau^2} \quad (3.13)$$

which indicates that scattering would have little effect on the interactions unless the rate was comparable to  $\omega_p$  since the relevant values of  $\omega$  are of order  $\omega_p$  or higher.

#### IV. DISPERSION FORCES IN THE WIGNER CRYSTAL

The pseudoatom interaction derived in Sec. II is characterized by an energy scale identified with collective modes, the plasmons, so it is of interest to determine whether the interaction is in fact mediated by these collective modes. In this section and the next we argue that this is indeed the case by computing the finite temperature corrections to the zero-temperature results, both for pseudoatoms and for the Wigner crystal. These corrections are exponential in the quantity  $\hbar\omega_p/k_B T$ , suggesting the interactions arise from the excitations of plasmons.

In the Wigner crystal, the low-density state of the electron gas which we consider in this section, the same van der Waals interactions appear, this time arising from "real" atoms, since the electrons are localized within lattice cells. We shall consider a simplified description of the Wigner crystal in which each of the lattice sites is surrounded by a spherical unit cell of uniform compensating background, rather than the actual Wigner-Seitz cell appropriate to the given lattice structure. Each such unit cell behaves like an atom with deviations of the electron coordinate from the center of the cell creating instantaneous dipoles which then polarize nearby cells, leading to van der Waals forces. The particularly simple form of these "elementary excitations" of the system leads to an analytic study of pseudoatom interactions at both zero and finite temperature, with the results at  $T = 0$  being nearly identical to those found in Sec. II in the limit of high electron number densities, and to those in the following section for  $T > 0$ .

Consider two well-separated, uniformly charged spheres containing one electron each, and let the number density of the uniform positive background be  $\rho$ , so that each of their radii  $R$  satisfies

$$\frac{4\pi}{3} \rho R^3 = 1. \quad (4.1)$$

An elementary electrostatic calculation shows that the electron inside each sphere is subjected to a harmonic potential with characteristic frequency  $\omega_p$  when it deviates from the center of the cell, where

$$\omega_p^2 = \frac{4\pi\rho e^2}{3m}, \quad (4.2)$$

while the residual interaction due to the electrostatic potential between the two spheres is

$$\mathcal{H}_{\text{int}} = \frac{e^2}{r} + \frac{e^2}{|\mathbf{r} + \mathbf{r}_1 - \mathbf{r}_2|} - \frac{e^2}{|\mathbf{r} - \mathbf{r}_2|} - \frac{e^2}{|\mathbf{r} + \mathbf{r}_1|} \quad (4.3)$$

where  $\mathbf{r}$  is the distance between the centers of the two spheres and  $\mathbf{r}_1, \mathbf{r}_2$  are the local electron deviations from the centers of the corresponding spheres, as illustrated in Fig. 4 for a two-dimensional lattice. Expanding  $\mathcal{H}_{\text{int}}$  in powers of  $1/r$  we obtain the familiar leading order contribution

$$\mathcal{H}_{\text{int}} \approx \frac{e^2}{r^5} [r^2(\mathbf{r}_1 \cdot \mathbf{r}_2) - 3(\mathbf{r} \cdot \mathbf{r}_1)(\mathbf{r} \cdot \mathbf{r}_2)]. \quad (4.4)$$

For computational purposes, it is convenient to choose the  $z$  axis parallel to the vector  $\mathbf{r}$ . The total Hamiltonian is then the sum of the kinetic and potential energy of the electrons in the presence of the compensating background,

$$\mathcal{H} \approx \frac{\mathbf{p}_1^2}{2m} + \frac{\mathbf{p}_2^2}{2m} + \frac{1}{2} m\omega_p^2 (\mathbf{r}_1^2 + \mathbf{r}_2^2) + \frac{e^2}{r^3} [x_1 x_2 + y_1 y_2 - 2z_1 z_2]. \quad (4.5)$$

Since this Hamiltonian is quadratic in the electron coordinates it be diagonalized exactly. First note that  $\mathcal{H}$  is the sum of three decoupled one dimensional Hamiltonians of the form

$$h_\mu = \frac{p_{1,\mu}^2}{2m} + \frac{p_{2,\mu}^2}{2m} + a_\mu (r_{1,\mu}^2 + r_{2,\mu}^2) + 2b_\mu r_{1,\mu} r_{2,\mu}, \quad (4.6)$$

for  $\mu = x, y, z$ . Defining the collective coordinates  $\xi_{1,\mu} \equiv (r_{1,\mu} + r_{2,\mu})/\sqrt{2}$  and  $\xi_{2,\mu} \equiv (r_{1,\mu} - r_{2,\mu})/\sqrt{2}$  and their conjugate momenta  $\pi_{1,\mu} \equiv (p_{1,\mu} + p_{2,\mu})/\sqrt{2}$  and  $\pi_{2,\mu} \equiv (p_{1,\mu} - p_{2,\mu})/\sqrt{2}$ , the individual Hamiltonians become

$$h_\mu = \frac{\pi_{1,\mu}^2}{2m} + \frac{\pi_{2,\mu}^2}{2m} + (a_\mu + b_\mu) \xi_{1,\mu}^2 + (a_\mu - b_\mu) \xi_{2,\mu}^2. \quad (4.7)$$

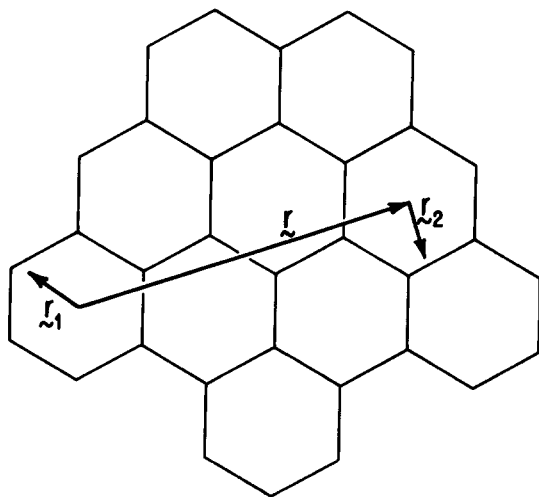


FIG. 4. Coordinates describing interactions between two unit cells in the two-dimensional Wigner crystal.

The energy levels of this system may be labeled by two quantum numbers,  $n$  and  $m$ ,

$$E_{n,m} = \epsilon_+ (n + \frac{1}{2}) + \epsilon_- (m + \frac{1}{2}), \quad (4.8)$$

where

$$\epsilon_\pm = \hbar [2(a_\mu \pm b_\mu)/m]^{1/2}. \quad (4.9)$$

In the three-dimensional case at hand we find that the exact energy levels depend on six quantum numbers  $k_1, k_2, l_1, l_2, m_1, m_2$ , and can be written

$$E = \alpha_+ (k_1 + l_1 + 1) + \alpha_- (k_2 + l_2 + 1) + \gamma_+ (m_1 + \frac{1}{2}) + \gamma_- (m_2 + \frac{1}{2}), \quad (4.10)$$

where

$$\alpha_\pm = \hbar \left( \omega_p^2 \pm \frac{e^2}{mr^3} \right)^{1/2}, \quad \gamma_\pm = \hbar \left( \omega_p^2 \pm 2 \frac{e^2}{mr^3} \right)^{1/2}. \quad (4.11)$$

The partition function  $Z = \text{Tr} \exp\{-\beta E\}$  is found to be

$$Z = \exp[-\beta(\alpha_+ + \alpha_-) + (\gamma_+ + \gamma_-)/2] \times (1 - e^{-\beta\alpha_+})^{-2} (1 - e^{-\beta\alpha_-})^{-2} \times (1 - e^{-\beta\gamma_+})^{-1} (1 - e^{-\beta\gamma_-})^{-1}. \quad (4.12)$$

from which the total energy of the system,

$$\langle H \rangle_T = - \left( \frac{\partial \log Z}{\partial \beta} \right),$$

is

$$\langle H \rangle_T = 3\hbar\omega_p + 6 \frac{\hbar\omega_p}{e^{2\zeta} - 1} + \phi(r), \quad (4.13)$$

where, expanding to second order in  $e^2/(mr^3\omega_p^2)$  we obtain the long-range temperature-dependent pair interaction

$$\phi(r) \approx -\frac{3}{4} \hbar\Delta(T) \left( \frac{e^2}{m\omega_p^2} \right)^2 \frac{1}{r^6}. \quad (4.14)$$

Here, the temperature-dependent excitation energy, shown in Fig. 5, is

$$\Delta(T) = \omega_p \left[ \coth(\zeta) + \frac{\zeta}{\sinh^2(\zeta)} - 2 \coth(\zeta) \frac{\zeta^2}{\sinh^2(\zeta)} \right], \quad (4.15)$$

where  $\zeta = \beta\hbar\omega_p/2$ .

At zero temperature, where  $\Delta(0) = \omega_p$ , and with the apparent static polarizability  $\alpha(0) = e^2/m\omega_p^2 = 3/4\pi\rho$ , we see that Eq. (4.14) is essentially of the pseudoatom form found in Eq. (2.32), except for the difference in the bulk and radial plasmon frequencies. The leading finite-temperature corrections to the ground-state excitation frequency take the form

$$\Delta(T) \approx \omega_p \left[ 1 - 2 \left( \frac{\hbar\omega_p}{k_B T} \right)^2 \exp(-\hbar\omega_p/k_B T) + \dots \right], \quad (4.16)$$

signifying that the interactions are mediated by the exchange of virtual excitations of energy  $\hbar\omega_p$ , that is by the exchange of virtual radial plasmons. At temperatures large compared to the plasmon energy, the excitation frequency rapidly decays,

$$\Delta(T) \simeq \omega_p \frac{(\hbar\omega_p/k_B T)^3}{45}, \quad (4.17)$$

vanishing in the limit of infinite temperature.

It may be readily verified that the value of the static polarizability  $\alpha(0) = 3/4\pi\rho$  is fully consistent with the formal definition of  $\alpha(\omega)$  in Eq. (2.14). Within the spherical approximation to the Wigner-Seitz cells we know that the energy levels of the atoms in the Wigner crystal are those of an ideal three-dimensional harmonic oscillator, so the matrix elements that enter Eq. (2.14) obey the usual selection rules of only connecting adjacent states in the ladder of oscillator levels. Using the isotropy of space, we find the ground state polarizability to be

$$\alpha(\omega) = \frac{2}{3} \frac{e^2}{\hbar} 3 \frac{\omega_p |\langle 1|\hat{x}|0\rangle|^2}{\omega_p^2 - \omega^2}, \quad (4.18)$$

the operator  $\hat{x}$  being that for the  $x$ -coordinate of position. The matrix element  $\langle 1|\hat{x}|0\rangle$  is readily evaluated as  $(\hbar/2m\omega_p)^{1/2}$ , yielding  $\alpha(\omega)$  as above.

The cohesive energy per electron in the Wigner crystal is the sum of the zero-point energy per particle and the contribution of the pair interaction, Eq. (4.14), from all other sites in the lattice. For a body-centered-cubic lattice, for instance, in which the density  $\rho$  and nearest-neighbor distance  $d$  are related by  $\rho = 3\sqrt{3}/4d^3$ , we obtain

$$E = \frac{e^2}{2a_0} \left( 3 - \frac{A_6}{4\pi^2} \right) r_s^{-3/2}, \quad (4.19)$$

where  $A_6 \simeq 12.25$  is the Madelung constant for a bcc lattice

with an interaction decaying as  $r^{-6}$ , and  $4\pi r_s^3/3 = 1/a_0^3\rho$ . The coefficient in parentheses in Eq. (4.19) has a value 2.69, close to that of Carr<sup>23</sup> (2.66) who proceeded by determining the collective excitations of the Wigner crystal. These results imply that at least in the Wigner crystal, the van der Waals interaction accounts for much of the cohesive energy. Note that in the high density limit, the interactions we have been discussing are between pseudoatoms centered about point ions, whereas in the Wigner crystal the interactions are between single electrons in their Wigner-Seitz cells of uniform background charge, so there may not be any continuous link between the two systems. However, the presence of these van der Waals interactions in both systems, with similar forms for the effective polarizabilities, does suggest that the same interaction should be present at all intermediate densities of the electron gas.

## V. PSEUDOATOM INTERACTIONS AT FINITE TEMPERATURE

The interpretation of the pseudoatom dispersion interaction as a plasmon-mediated one is lent support by a computation of the finite-temperature generalization of the zero-temperature results of the previous section. We show here that such corrections at low temperature are exponential in the quantity  $\hbar\omega_p/k_B T$ , as one might expect from the presence of an energy gap of  $\hbar\omega_p$  in the plasmon excitation spectrum, analogous to the gap in the Wigner crystal.

The generalization of the zero-temperature pseudoatom interaction Eq. (2.23) to finite temperatures is

$$\begin{aligned} \Phi_{2 \text{ pseudo}}(r) = & -\frac{1}{\beta} \sum_{\omega} \int \frac{d^3q}{(2\pi)^3} \int \frac{d^3q'}{(2\pi)^3} e^{-i(\mathbf{q}-\mathbf{q}')\cdot\mathbf{R} - i(\mathbf{q}'-\mathbf{q})\cdot\mathbf{R}'} \left[ \frac{e^4 \hat{v}_{ps}(|\mathbf{q}-\mathbf{q}'|)}{\hbar^2 \epsilon(|\mathbf{q}-\mathbf{q}'|,0)} \frac{\mathcal{F}(\mathbf{q}'-\mathbf{q},0,\mathbf{q},i\omega, -\mathbf{q}', -i\omega)}{\epsilon(\mathbf{q},i\omega)} \right] \\ & \times \left[ \frac{e^4 \hat{v}_{ps}(|\mathbf{q}'-\mathbf{q}|)}{\hbar^2 \epsilon(|\mathbf{q}'-\mathbf{q}|,0)} \frac{\mathcal{F}(\mathbf{q}-\mathbf{q}',0, -\mathbf{q}, -i\omega, -\mathbf{q}', i\omega)}{\epsilon(\mathbf{q}',i\omega)} \right] \hat{v}_c(q) \hat{v}_c(q'), \end{aligned} \quad (5.1)$$

where the sum on  $\omega$  is over the Matsubara frequencies  $\omega_l = (2l+1)\pi/\beta\hbar$  and  $\epsilon$  is now a finite-temperature dielectric function.

The finite-temperature three-point function  $\mathcal{F}$  itself may be written in terms of the thermal Green's functions  $\mathcal{G}^0(\mathbf{k},\omega_n) = (i\omega_n - \omega_{\mathbf{k}})^{-1}$ , with  $\omega_{\mathbf{k}} = (\epsilon_{\mathbf{k}} - \mu)/\hbar$ , as

$$\begin{aligned} \mathcal{F}(\mathbf{q}_1, i\omega_1, \mathbf{q}_2, i\omega_2, -\mathbf{q}_1 - \mathbf{q}_2, -i\omega_1 - i\omega_2) = & 2 \int \frac{d^3k}{(2\pi)^3} \sum_{\omega} [\mathcal{G}^0(\mathbf{k},\omega) \mathcal{G}^0(\mathbf{k} + \mathbf{q}_2, \omega + \omega_2) \mathcal{G}^0(\mathbf{k} + \mathbf{q}_1, \omega - \omega_1) \\ & + \mathcal{G}^0(\mathbf{k},\omega) \mathcal{G}^0(\mathbf{k} - \mathbf{q}_2, \omega - \omega_2) \mathcal{G}^0(\mathbf{k} + \mathbf{q}_1, \omega + \omega_1)]. \end{aligned} \quad (5.2)$$

Using the standard representation of the Matsubara sum as a contour integral over the Fermi-Dirac distribution function, and then taking the high-frequency limit of the result, we find, for instance, that the second term of  $\mathcal{F}$  in Eq. (5.2) is, with  $\omega_1 = -\omega_2 = \omega$ ,

$$\begin{aligned} \frac{2\beta\hbar}{(i\omega)^2} \int \frac{d^3k}{(2\pi)^3} \frac{\omega_{\mathbf{k}+\mathbf{q}_1} - \omega_{\mathbf{k}}}{\omega_{\mathbf{k}+\mathbf{q}_1} - \omega_{\mathbf{k}-\mathbf{q}_2}} \\ \times [n(|\mathbf{k}-\mathbf{q}_2|) - n(|\mathbf{k}+\mathbf{q}_1|)], \end{aligned} \quad (5.3)$$

where  $n(\mathbf{k}) = \{1 + \exp[\beta(\epsilon_{\mathbf{k}} - \mu)]\}^{-1}$  is the Fermi-Dirac distribution function. The explicit leading-order dependence of Eq. (5.3) on the vectors  $\mathbf{q}_1$  and  $\mathbf{q}_2$  may be ob-

tained by expanding the frequencies  $\omega_{\mathbf{k}}$  in Eq. (5.3), yielding

$$\frac{2\beta\hbar}{(i\omega)^2} (\mathbf{q}_1 \cdot \mathbf{q}_2) \int \frac{d^3k_1}{(2\pi)^3} \frac{n(|\mathbf{k}_1 - \mathbf{p}|) - n(\mathbf{k}_1)}{p^2 - 2\mathbf{k}_1 \cdot \mathbf{p}} \quad (5.4)$$

where  $\mathbf{p} = \mathbf{q}_1 + \mathbf{q}_2$ . Systematic expansion of this for small  $\mathbf{p}$  then yields the result

$$\mathcal{F}(\mathbf{q}_1, \omega, \mathbf{q}_2, -\omega, -\mathbf{q}_1 - \mathbf{q}_2, 0) = \frac{2\beta\hbar^2 \chi_{\mu}(0)}{m\lambda_T^3} \frac{(\mathbf{q}_1 \cdot \mathbf{q}_2)}{\omega^2}, \quad (5.5)$$

where

$$\chi_\mu(x) = \frac{1}{\pi x} \int_0^\infty d\xi \frac{\xi}{1 + \exp(\xi^2/4\pi - \beta\mu)} \log \left| \frac{2\xi + x}{2\xi - x} \right|. \quad (5.6)$$

As in the case for  $T = 0$ , the contribution to  $\Phi$  from the statically screened Coulomb lines connecting the ions to the three-point functions is obtained as the  $q \rightarrow 0$  limit of the ratio  $v_{ps}(q)/\epsilon(q,0)$ , namely  $4\pi/k_{sc}^2$ . In this case,

$$k_{sc}^2 = \lim_{q \rightarrow 0} q^2 \epsilon(q,0) = - \lim_{q \rightarrow 0} 4\pi \Pi(q,0), \quad (5.7)$$

where we have used the relation between the dielectric function and the polarizability insertion  $\Pi$ . This in turn gives<sup>24</sup>

$$k_{sc}^2 = 8\pi\beta e^2 \lambda_T^{-3} \chi_\mu(0), \quad (5.8)$$

where  $\lambda_T = 2\pi\beta\hbar^2/m$  is the thermal wavelength of the electrons, and  $\chi_\mu$  is given in Eq. (5.6). Substitution back into Eq. (5.2) shows there to be a complete cancellation of the function  $\chi_\mu$ , with the result

$$\Phi_{2\text{pseudo}}(r) = - \frac{3}{4} \left( \frac{1}{4\pi\rho} \right)^2 \frac{\hbar\Delta(T)}{r^6}, \quad (5.9)$$

that is to say, a pseudoatom interaction having the same form as the result at  $T = 0$ , except that the apparent excitation frequency is temperature dependent,

$$\Delta(T) = \frac{4}{\beta\hbar} \sum_n \left( \frac{\omega_p^2}{\omega_n^2 + \omega_p^2} \right)^2 = \omega_p [\tanh(\zeta) - \zeta \operatorname{sech}^2(\zeta)], \quad (5.10)$$

where  $\zeta = \hbar\omega_p/2k_B T$  is the same dimensionless variable that appeared in the study of the Wigner crystal in Sec. IV.

As in the case of the Wigner crystal,  $\Delta(T)$  for pseudoatoms exhibits exponentially small low-temperature corrections; i.e., for  $k_B T \ll \hbar\omega_p$ , one obtains

$$\Delta(T) \simeq \omega_p \left[ 1 - 4 \left( \frac{\hbar\omega_p}{k_B T} \right) \exp(-\hbar\omega_p/k_B T) + \dots \right], \quad (5.11)$$

whereas in the opposite limit of high temperatures,

$$\Delta(T) \simeq \frac{1}{48} \omega_p \left( \frac{\hbar\omega_p}{k_B T} \right)^3, \quad (5.12)$$

again, remarkably similar to the Wigner crystal results Eqs. (4.16) and (4.17). The full temperature dependence of  $\Delta(T)$  is shown in Fig. 5. In both cases the plasmon frequency is the important energy scale, even though in the pseudoatom case it is purely a collective mode, and not associated with local electronic excitations, as in the case of the Wigner crystal.

## VI. DISCUSSION: IMPLICATIONS FOR CRITICAL PHENOMENA IN METALLIC FLUIDS

In discussing the relationship between critical phenomena in fluids on the one hand, in which there is a broken symmetry between liquid and vapor, and statistical mechanical models exhibiting exact symmetries between thermodynamic functions in coexisting phases on the other, it has been found useful to focus on the nonuniversal critical amplitudes of thermodynamic singularities.<sup>11</sup> In particular, the order parameter  $\Delta\rho = (\rho_l - \rho_v)/2\rho_c$  and the diameter

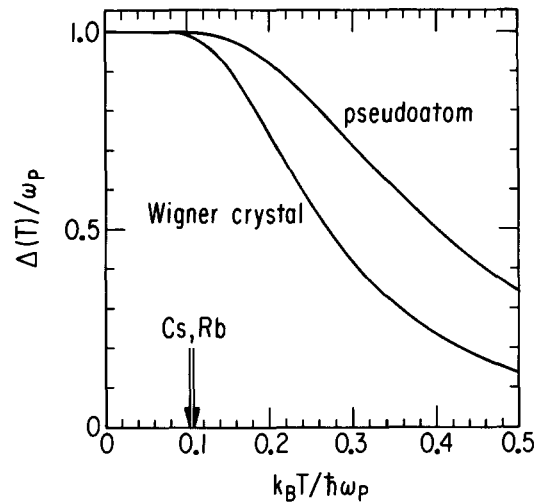


FIG. 5. Temperature-dependent apparent excitation energies of interacting pseudoatoms and in the Wigner crystal. Also shown are the locations of the critical points of cesium and rubidium.

$\rho_d = (\rho_l + \rho_v)/2\rho_c$ , where  $\rho_l$  and  $\rho_v$  are the liquid and vapor phase densities, respectively, define the amplitudes  $A_1$ ,  $A_{1-\alpha}$  and  $A_\beta$  near the critical point:

$$\begin{aligned} \Delta\rho &\simeq A_\beta t^\beta + \dots, \\ \rho_d &\simeq 1 + A_{1-\alpha} t^{1-\alpha} + A_1 t + \dots \end{aligned} \quad (6.1)$$

where  $t = |(T - T_c)/T_c|$  is the reduced temperature and  $\alpha$  is the specific heat exponent. Thus, the amplitude  $A_\beta$  determines the width of the coexistence curve;  $A_1$  and  $A_{1-\alpha}$  determine the skewing of the liquid-vapor phase boundary. The singular term in the mean density, with the nonclassical exponent  $1 - \alpha$ , is known from studies of certain lattice models and field theories,<sup>11</sup> and can appear in systems which lack perfect symmetry between liquid and vapor.

Recent work on three-body forces in insulating fluids<sup>9,10</sup> has suggested that these critical amplitudes for the density depend strongly on the relative magnitude of the three-body potential, increasing monotonically with the critical polarizability product  $\alpha(0)\rho_c$ , the value of which typically falls in the range 0.003–0.02 for those fluids. In the pseudoatom picture, we find  $\alpha(0)\rho_c \simeq 1/4\pi \simeq 0.08$  in the high-density limit, implying that the three-body forces are relatively more important by perhaps as much as an order of magnitude. While the critical densities of the metallic fluids are not within the high-density limit which defines the strict domain of validity of the pseudoatom picture as derived above, we may expect qualitatively the pseudoatom polarizability to remain large even at somewhat lower densities, giving rise to extremely broad and asymmetric coexistence curves, the sign of the asymmetry being like that in insulating fluids since the underlying (predominantly repulsive) Axilrod-Teller form of the triplet interaction is unchanged. Indeed, as indicated in Fig. 1, this is the case in metallic fluids. Detailed analysis<sup>16</sup> of the amplitudes, while complicated by the limited range of reduced temperatures accessible, indicates rough consistency with what is implied by the pseudoatom polarizability.

Finally, we turn to the question of the origin of the ener-

gy scale of the critical point in metallic fluids. Consider first a van der Waals<sup>3</sup> description of the relation between the equation of state and the intermolecular potential  $\phi(r)$ , which is itself partitioned into repulsive and attractive contributions  $\phi_0$  and  $\phi_1$ , respectively. The pressure  $P(\rho, T)$  may be approximated as that of the repulsive reference system plus a mean field contribution from the attractive interactions,

$$P(\rho, T) = P_0(\rho, T) - a\rho^2, \quad a = -\frac{1}{2}\hat{\phi}_1(0), \quad (6.2)$$

where  $\hat{\phi}_1(k)$  is the Fourier transform of  $\phi_1$ . With the reference pressure typically purely entropic,  $P_0 \simeq k_B T p_0(\rho)$ , and  $a$  independent of  $T$  for conventional dispersion forces, Eq. (6.2) implies that isochores in the  $P$ - $T$  plane are straight lines. Recent experiments by Hensel *et al.*<sup>16</sup> have shown linear isochores for cesium and rubidium near the critical point, where the fluids are still metallic. The coefficient  $p_0(\rho)$  obtained from the data has a density dependence that supports its interpretation as a hard-sphere-like entropy. Unlike in insulating fluids, however, the van der Waals parameter  $a$  determined from the extrapolated pressure at  $T=0$  has a strong density dependence, varying over two decades in density as  $\rho^{-1}$ . This is in marked contrast to the density-independence that would be expected for real fluctuating-dipole interactions. Now Eq. (6.2) itself was derived assuming the interactions were independent of density. It may be modified for a charged system (using the compressibility sum rule) to obtain a relationship between the integrated strength of the attractive part of the effective ion-ion potential and the long-wavelength properties of the electron gas. Note also that even if most of the pressure is provided by the electrons, we may formally express  $P$  in terms of the effective ion-ion potential because of the requirement of charge neutrality.

When there is a single length scale  $\sigma$  associated with the potential (e.g., the short-distance cutoff of  $\phi_1$ ) we may expect the basic results of the classical theory of the critical point to hold; The thermal energy  $k_B T_c$  scales as  $a/\sigma^3$ , with  $a \sim \hbar \Delta \alpha(0)^2 \sigma^{-3}$  for dispersion forces, and  $\rho_c \simeq \sigma^{-3}$ . This yields the central relation

$$\frac{k_B T_c}{\hbar \Delta} \sim [\alpha(0)\rho_c]^2. \quad (6.3)$$

In the context of a pseudoatom model of the critical point, for which the polarizability product is a pure number,  $\alpha_{\text{pseudo}}(0)\rho_c \simeq 0.08$ , we are then led to the prediction

$$\frac{k_B T_c}{\hbar \omega_p} \simeq \text{constant}. \quad (6.4)$$

This is consistent with the experimental  $k_B T_c / \hbar \omega_p(\rho_c) = 0.103 \pm 0.002$ , and  $0.108 \pm 0.002$ , for Cs and Rb, respectively, which, as shown in Fig. 5, fall within the domain of the zero-temperature pseudoatom theory.

To assess the possible relevance of the pseudoatom interactions to the observation  $a(\rho) \sim \rho^{-1}$  it is necessary to determine the characteristic short-range cutoff on this interaction which renders the Fourier transform  $\hat{\phi}_1(0)$  finite. Returning to the high-frequency approximation to the three-point function of the electron gas, one can show that its

breakdown occurs for wave vectors on the order of the Thomas-Fermi momentum  $q_{TF} \sim \rho^{-1/6}$ . Clearly, at distances less than the screening length the effective ionic interaction will have a large repulsive component due to the direct Coulomb interaction. These considerations suggest a real-space cutoff to the pseudoatom potential at a distance proportional to the screening length, which is the effective size of the density inhomogeneity that defines the pseudoatom. With the cutoff  $\sigma$  scaling as  $\rho^{-1/6}$ , we find

$$\hat{\phi}_{2\text{pseudo}}(0) \sim \omega_p \alpha(0)^2 \sigma^{-3} \sim \rho^{1/2} \rho^{-2} \rho^{1/2} \sim \rho^{-1}, \quad (6.5)$$

as seen in experiment.

These considerations illustrate that the pseudoatom picture of metallic fluids discussed in this work may provide a qualitative explanation of some of the interesting differences between the critical properties of fluid metals and those of typical insulating fluids. Under the approximations explored here, the metallic systems behave as if they were insulating fluids, but with a large and density-dependent polarizability  $\alpha_{\text{pseudo}}(\omega)$ , and associated two-, three-, and many-body interactions which have a much larger relative magnitude than is found in typical insulating systems. The energy scale of importance is the plasma frequency  $\omega_p$ , as is illustrated both in the magnitude of the interactions, and in their temperature dependence. This leads to the suggestion that the correlated fluctuations in the screening clouds associated with the interactions are actually determined by the exchange of virtual plasmons. The fact that nearly the same type of interparticle interactions appears in both metallic and insulating fluids, with a van der Waals form scaling as  $r^{-6}$  at long range, suggests that it may be of use in studying certain properties of these systems near the metal-insulator transition.

Several important questions remain for future work. The high-frequency approximation we have made in calculating the interaction is not entirely satisfactory, since it neglects a logarithmic factor found in Ref. 15, and to the extent that the interaction is not precisely of the form  $1/r^6$ , the analogy with polarizable insulators is less complete. We have also not shown a direct connection between the plasma oscillations and the fluctuating pseudoatoms, although Ref. 15 does demonstrate that such a connection can be found in a phenomenological model. As discussed elsewhere,<sup>25</sup> we have found that the  $1/r^6$  potential may be derived from a generalized Thomas-Fermi picture of the screening cloud around an impurity, with the interaction itself arising from quantization of the plasma oscillations. Since we have been concerned with the long range properties of the interactions, we also can not give a precise numerical value for the integrated strength of the potential, although using the screening length as a cutoff scale reproduces the observed density dependence. Nevertheless, this concept of fluctuating pseudoatoms presents a novel way of thinking about metallic fluids and their long-range interactions, one which may prove useful in understanding many of the similarities and differences between the thermodynamics of metals and insulators.

## ACKNOWLEDGMENTS

We are grateful to N. W. Ashcroft, F. Hensel, B.Y.-K. Hu, A. C. Maggs, S. A. Rice, and N. S. Wingreen for exten-

sive discussions, to N. W. Ashcroft and G. F. Mazenko for detailed comments on the manuscript, and to F. Hensel for communication of results prior to publication. This work was supported in part by the National Science Foundation, through Grant No. DMR-87-15590 and the Materials Science Center at Cornell University, and No. DMR85-19460 through the Materials Research Laboratory at the University of Chicago, and by a Robert McCormick Postdoctoral Fellowship (R.E.G.).

- <sup>1</sup>R. E. Goldstein and N. W. Ashcroft, *Phys. Rev. Lett.* **55**, 2164 (1985).
- <sup>2</sup>D. Sluis and S. A. Rice, *J. Chem. Phys.* **79**, 5658 (1983).
- <sup>3</sup>J. S. Rowlinson and B. Widom, *Molecular Theory of Capillarity* (Oxford, New York, 1982), p. 16.
- <sup>4</sup>M. P. d'Evelyn and S. A. Rice, *Phys. Rev. Lett.* **47**, 1844 (1981); *J. Chem. Phys.* **78**, 5081, 5225 (1983).
- <sup>5</sup>F. Hensel, S. Jüngst, B. Knuth, H. Uchtmann, and M. Yao, *Physica B* **139/140**, 90 (1986); and (private communication).
- <sup>6</sup>S. Jüngst, B. Knuth, and F. Hensel, *Phys. Rev. Lett.* **55**, 2160 (1985).
- <sup>7</sup>B. Wallace, Jr. and H. Meyer, *Phys. Rev. A* **2**, 1563 (1970).
- <sup>8</sup>E. A. Guggenheim, *J. Chem. Phys.* **13**, 253 (1945).
- <sup>9</sup>R. E. Goldstein, A. Parola, N. W. Ashcroft, M. W. Pestak, M. H. W. Chan, J. R. de Bruyn, and D. A. Balzarini, *Phys. Rev. Lett.* **58**, 41 (1987); M. W. Pestak, R. E. Goldstein, M. H. W. Chan, J. R. de Bruyn, D. A. Balzarini, and N. W. Ashcroft, *Phys. Rev. B* **36**, 599 (1987); R. E. Goldstein and A. Parola, *Phys. Rev. A* **35**, 4770 (1987).
- <sup>10</sup>R. E. Goldstein and A. Parola, *J. Chem. Phys.* **88**, 7059 (1988).
- <sup>11</sup>For a survey of the history of the singular diameter, see, e.g., R. E. Goldstein and A. Parola, *Acc. Chem. Res.* **22**, 77 (1989).
- <sup>12</sup>B. M. Axilrod and E. Teller, *J. Chem. Phys.* **11**, 299 (1943).
- <sup>13</sup>For an early discussion of the notion of pseudoatoms, see J. M. Ziman, *The Physics of Metals. 1. Electrons* (Cambridge University, Cambridge, 1969), p. 258.
- <sup>14</sup>A. C. Maggs and N. W. Ashcroft, *Phys. Rev. Lett.* **59**, 113 (1987).
- <sup>15</sup>D. C. Langreth and S. H. Vosko, *Phys. Rev. Lett.* **59**, 497 (1987); see also D. C. Langreth, in *Proceedings of the A. J. Coleman Symposium, 1985*, edited by R. Ehrdal and V. Smith (Riedel, Dordrecht, 1987).
- <sup>16</sup>R. E. Goldstein, A. P. Smith, and A. Parola, S. Jüngst, B. Knuth, and F. Hensel (to be submitted).
- <sup>17</sup>K. K. Mon, N. W. Ashcroft, and G. V. Chester, *Phys. Rev. B* **19**, 5103 (1979).
- <sup>18</sup>J. J. Rehr, E. Zaremba, and W. Kohn, *Phys. Rev. B* **12**, 2062 (1975).
- <sup>19</sup>J. Mahanty and R. Taylor, *Phys. Rev. B* **17**, 554 (1978).
- <sup>20</sup>A. Fetter and J. D. Walecka, *Quantum Theory of Many-Particle Systems* (McGraw-Hill, New York, 1971).
- <sup>21</sup>See also a related discussion in B.Y.-K. Hu and J. W. Wilkins, *Phys. Rev. B* (to be published).
- <sup>22</sup>E. M. Lifshitz and L. P. Pitaevskii, *Physical Kinetics* (Pergamon, New York, 1981), p. 117.
- <sup>23</sup>W. J. Carr, Jr., *Phys. Rev.* **122**, 1437 (1961).
- <sup>24</sup>See, Ref. 20, p. 277.
- <sup>25</sup>A. Parola, R. E. Goldstein, and A. P. Smith (to be submitted).